Achieving Seventh-Order Amplitude Accuracy in Leapfrog Integrations

PAUL D. WILLIAMS

Department of Meteorology, University of Reading, Reading, United Kingdom

ABSTRACT

The leapfrog time-stepping scheme makes no amplitude errors when integrating linear oscillations. Unfortunately, the Robert–Asselin filter, which is used to damp the computational mode, introduces first-order amplitude errors. The Robert–Asselin–Williams (RAW) filter, which was recently proposed as an improvement, eliminates the first-order amplitude errors and yields third-order amplitude accuracy. However, it has not previously been shown how to further improve the accuracy by eliminating the third- and higher-order amplitude errors. Here, it is shown that leapfrogging over a suitably weighted blend of the filtered and unfiltered tendencies eliminates the third-order amplitude errors and yields fifth-order amplitude accuracy. It is further shown that the use of a more discriminating $(1, -4, 6, -4, 1)$ filter instead of a $(1, -2, 1)$ filter eliminates the fifth-order amplitude errors and yields seventh-order amplitude accuracy. Other related schemes are obtained by varying the values of the filter parameters, and it is found that several combinations offer an appealing compromise of stability and accuracy. The proposed new schemes are tested in numerical integrations of a simple nonlinear system. They appear to be attractive alternatives to the filtered leapfrog schemes currently used in many atmosphere and ocean models.

1. Introduction

A growing body of evidence demonstrates that atmospheric and oceanic simulations are sensitive to the time-stepping method (e.g., Pfeffer et al. 1992; Huang and Pedlosky 2003; Zhao and Zhong 2009) and to the time-step size (e.g., Williamson and Olson 2003; Heimsund and Berntsen 2004; Teixeira et al. 2007; Mishra et al. 2008). For example, in simulations of tropical climate with the Community Atmosphere Model version 3 (CAM3), Mishra and Sahany (2011) report that changing the time-step size changes the Kelvin wave speed and the convective and stratiform precipitation. Furthermore, in a simplified atmosphere general circulation model, Amezcua (2012) reports that the sensitivity of the skill of medium-range weather forecasts to the time-stepping method is about the same as it is to the physics parameterizations.

A popular time-stepping method is the second-order centered-difference scheme, which is affectionately known as the leapfrog scheme (e.g., Haltiner and Williams 1980; Durran 1999; Kalnay 2003; Jablonowski and Williamson 2011). When integrating linear oscillations, the leapfrog scheme introduces second-order phase errors into the numerical solution after a given time interval, but the amplitude errors are exactly zero [assuming the Courant–Friedrichs–Lewy (CFL) stability condition is satisfied]. The leapfrog scheme possesses a $2\Delta t$ computational mode, which can cause the numerical solution at even and odd time steps to split apart unphysically (e.g., Lilly 1965; Young 1968; Mesinger and Arakawa 1976). Various methods have been proposed to control the time-splitting instability (e.g., Kurihara 1965; Magazenkov 1980; Dietrich and Wormeck 1985; Roache and Dietrich 1988), the most common being to apply the $(1, -2, 1)$ filter conceived by Robert (1966) and analyzed by Asselin (1972). The properties of the Robert–Asselin filter have been studied widely (e.g., Schlesinger et al. 1983; Déqué and Cariolle 1986; Tandon 1987; Robert and Lépine 1997; Cordero and Staniforth 2004; Marsaleix et al. 2012) and the filter is used extensively in current models (e.g., Griffies et al. 2001; Bartello 2002; Fraedrich et al. 2005; Hartogh et al. 2005; Williams et al. 2009).

The Robert–Asselin filter damps the computational mode by construction, but it also damps the physical mode and introduces first-order amplitude errors. To alleviate these problems, Williams (2009, 2011) proposed a simple modification known as the Robert–Asselin–Williams

Corresponding author address: Paul D. Williams, Department of Meteorology, University of Reading, Earley Gate, Reading RG6 6BB, United Kingdom.
E-mail: p.d.williams@reading.ac.uk

(RAW) filter. While the Robert–Asselin filter perturbs the state of the system only at the middle of the three time levels involved in the preceding leapfrog calculation, the RAW filter perturbs it additionally at the future time level. The two perturbations have opposite signs and, for the special case of equal magnitudes, the first-order amplitude errors are eliminated. The first-order damping vanishes, and the amplitude accuracy increases from first order to third order.

The RAW filter has been implemented, tested, and adopted in various models since it was proposed. It is the default time-stepping method in the atmosphere of the Model for Interdisciplinary Research on Climate version 5 (MIROC5; Watanabe et al. 2010). It is also the default time-stepping method in the Taiwan Multiscale Community Ocean Model (TIMCOM; Young et al. 2012), and it has been found to give ocean simulations that are in better agreement with observations in various important respects (Young et al. 2013). The RAW filter has been reported to improve both the spinup and the conservation energetics of the physical processes in an ice model, when used instead of the Robert–Asselin filter (Ren and Leslie 2011). It has been found to improve the skill of medium-range weather forecasts significantly when used instead of the Robert–Asselin filter in a simple atmospheric general circulation model (Amezcua et al. 2011). It has been implemented in a two-layer quasigeostrophic model of a rotating fluid (Oger et al. 2012). Finally, in semi-implicit integrations, it has been found to perform well in various respects compared to other semi-implicit methods (Durran and Blossey 2012; Clancy and Pudykiewicz 2013).

Are further improvements to the accuracy of the filtered leapfrog scheme possible? Can the third- and higher-order amplitude errors somehow be eliminated? Guidance is sought from Durran (1991), who proves a general proposition relating the order of the overall truncation error of any linear finite-difference time discretization to the order of the phase and amplitude errors in the numerical solution. The proposition shows that, for all second-order time-differencing schemes, the phase accuracy is exactly second order and the amplitude accuracy is at least third order. (These numbers refer to the error scaling after a given time interval, not after a single time step.) Note that the amplitude order of accuracy is unbounded from above and can be arbitrarily high, consistent with the unfiltered leapfrog scheme having an amplitude error of zero. The proposition suggests that the phase accuracy of filtered leapfrog schemes cannot be improved beyond second order, but the proposition does not rule out improving the amplitude accuracy beyond third order.

The goal of the present paper is to identify further possible improvements to the amplitude accuracy of the filtered leapfrog scheme. First, it is shown that leapfrogging over a suitably weighted blend of the filtered and unfiltered tendencies eliminates the third-order amplitude errors and yields fifth-order amplitude accuracy (section 2). Then, it is shown that the use of a more discriminating $(1, -4, 6, -4, 1)$ filter instead of a $(1, -2, 1)$ filter eliminates the fifth-order amplitude errors and yields seventh-order amplitude accuracy (section 3). Finally, the proposed new schemes are tested in numerical integrations of a simple nonlinear system (section 4). The paper concludes with a summary and discussion (section 5).

2. A composite-tendency leapfrog scheme

a. The numerical scheme

Consider filtered leapfrog integrations of the first-order ordinary differential equation:

$$\frac{dx}{dt} = f(x), \tag{1}$$

where t is time, $x(t)$ is the solution being sought, and $f(x)$ is a given function. We use a time step of size Δt and we write $x(n\Delta t) = x_n$ for any integer n. At each time step, the leapfrog calculation uses the tendency at the present time, n, to extrapolate the numerical solution forward by $2\Delta t$ from the past time, $n - 1$, to the future time, $n + 1$. It is assumed that a stabilizing filter then slightly perturbs the numerical solution at the present and future times, n and $n + 1$. Note that the numerical solution at the past time, $n - 1$, is not used in the subsequent leapfrog calculation. Therefore, the stability and accuracy of the scheme are unaffected by filter perturbations applied at time $n - 1$, and so without loss of generality the filter is assumed to perturb the numerical solution only at times n and $n + 1$. At the end of the integration, we will have calculated three numerical solutions at any time, m: x_m is the result of leapfrogging from $m - 2$ over $m - 1$ to reach m, $\overline{x}_m$ is the result of applying the filter immediately after leapfrogging from $m - 2$ over $m - 1$ to reach m, and $\overline{\overline{x}}_m$ is the result of applying the filter immediately after leapfrogging from $m - 1$ over m to reach $m + 1$.

In the usual implementation in computer codes, the filtered values immediately overwrite their predecessors in memory. Therefore, when leapfrogging from $n - 1$ over n to reach $n + 1$, at $n - 1$ we have access only to $\overline{\overline{x}}_{n-1}$ and not to $\overline{x}_{n-1}$ or x_{n-1}, and at n we have access only to $\overline{x}_n$ and not to x_n. Consequently, the usual implementation of the leapfrog calculation for (1) is

$$x_{n+1} = \bar{\bar{x}}_{n-1} + 2\Delta t f(\bar{x}_n). \tag{2}$$

However, if the predecessors are kept in memory instead of being overwritten, a possible alternative leapfrog scheme is

$$x_{n+1} = \bar{\bar{x}}_{n-1} + 2\Delta t[\gamma f(\bar{x}_n) + (1-\gamma)f(x_n)]. \tag{3}$$

Here, it is assumed we have access to x_n in addition to $\bar{x}_n$. The tendency in the leapfrog extrapolation is a composite tendency based on both. The weighting parameter is γ, which satisfies $0 \leq \gamma \leq 1$, and which determines whether the tendency is calculated only from x_n ($\gamma = 0$), only from $\bar{x}_n$ ($\gamma = 1$), or from a linear combination of the two. Note that $\bar{\bar{x}}_n$ cannot be included in the linear combination if the scheme is to remain explicit, because it is currently unknown and will be calculated only after the leapfrog step is done. The usual implementation in (2) is a special case of (3) when $\gamma = 1$, but the present section aims to analyze the effects of other values of γ.

The analysis will be done using the linear oscillation equation for the complex variable $x(t)$:

$$\frac{dx}{dt} = i\omega x, \tag{4}$$

where $i = \sqrt{-1}$ and ω is the real-valued angular frequency. The composite-tendency leapfrog scheme in (3) applied to the linear oscillation equation in (4) gives

$$x_{n+1} = \bar{\bar{x}}_{n-1} + 2i\omega\Delta t[\gamma \bar{x}_n + (1-\gamma)x_n]. \tag{5}$$

The RAW filter (Williams 2009, 2011) is

$$\bar{\bar{x}}_n = \bar{x}_n + \frac{\nu\alpha}{2}[\bar{\bar{x}}_{n-1} - 2\bar{x}_n + x_{n+1}], \tag{6}$$

$$\bar{x}_{n+1} = x_{n+1} - \frac{\nu(1-\alpha)}{2}[\bar{\bar{x}}_{n-1} - 2\bar{x}_n + x_{n+1}]. \tag{7}$$

The RAW filter parameters satisfy $0 \leq \nu \leq 1$ and $0 \leq \alpha \leq 1$, where ν specifies the strength of the filter and α determines the partitioning of the filter perturbations between times n and $n + 1$. The Robert–Asselin filter is recovered as a special case when $\alpha = 1$. Combining (3), (6), and (7) into a single equation for the numerical scheme demonstrates that, when $\nu \neq 0$ and for all values of γ, the overall truncation error is generally $O(\omega\Delta t)$, but becomes $O[(\omega\Delta t)^2]$ when $\alpha = \frac{1}{2}$. Therefore, the use of equal and opposite filter perturbations increases the overall accuracy from first order to second order.

To proceed with the linear oscillation analysis, the complex amplification factor, A, is defined by

$$A = \frac{x_{n+1}}{x_n} = \frac{\bar{x}_{n+1}}{\bar{x}_n} = \frac{\bar{\bar{x}}_{n+1}}{\bar{\bar{x}}_n}. \tag{8}$$

Writing (5)–(7) with function evaluations at time n only, using (8), yields a homogeneous matrix equation for the vector $(x_n, \bar{x}_n, \bar{\bar{x}}_n)$. For nontrivial solutions, the determinant of the 3×3 matrix of coefficients must vanish, yielding a cubic equation for the amplification factor:

$$c_3 A^3 + c_2 A^2 + c_1 A + c_0 = 0, \tag{9}$$

where

$$c_3 = 1, \tag{10}$$

$$c_2 = -\nu - [2 - \nu(1-\alpha)\gamma]i\omega\Delta t, \tag{11}$$

$$c_1 = -1 + \nu + \nu[2(1-\alpha)(1-\gamma) + \alpha]i\omega\Delta t, \tag{12}$$

$$c_0 = -\nu(1-\alpha)(1-\gamma)i\omega\Delta t. \tag{13}$$

Equation (9) generally yields three roots for $A(\nu, \alpha, \gamma, i\omega\Delta t)$. In addition to the physical mode, hereafter labeled P, there are generally two computational modes, hereafter labeled C1 and C2. However, when $\nu = 0$, $\alpha = 1$, or $\gamma = 1$, the cubic equation reduces to a quadratic equation (because $c_0 = 0$) and one of the computational modes vanishes. The additional computational mode arises because the use in (3) of x_n as well as $\bar{x}_n$ introduces an extra degree of freedom into the numerical scheme. The extra degree of freedom vanishes if $\gamma = 1$, because then x_n disappears from (3), and it vanishes if $\nu = 0$ or $\alpha = 1$, because then (7) implies that $x_n = \bar{x}_n$. The complex amplification factor for the exact solution is

$$A_{\text{exact}}(i\omega\Delta t) = \exp(i\omega\Delta t), \tag{14}$$

with a magnitude of $|A_{\text{exact}}| = 1$ and a phase of $\arg(A_{\text{exact}}) = \omega\Delta t$.

b. Behavior as $\omega\Delta t \rightarrow 0$

A series expansion for $|A_{\text{P}}|$ in powers of $\omega\Delta t$ is obtained using the symbolic manipulation capability of the Maple software (Maplesoft 2011). The amplitude error is thereby found to be

$$|A_{\text{P}}| - 1 = \frac{\nu(1-2\alpha)}{2(2-\nu)}(\omega\Delta t)^2 + O[(\omega\Delta t)^4]. \tag{15}$$

The leading-order amplitude error after taking a single time step generally scales as $(\Delta t)^2$. Therefore, the leading-order amplitude error compounded over $T/\Delta t$ time steps generally scales as Δt, implying first-order amplitude accuracy. The leading-order amplitude error is

approximately proportional to ν for $\nu \ll 1$. It is independent of γ, showing that the amplitude order of accuracy is generally insensitive to whether the leapfrog tendency is calculated from the filtered or unfiltered solution. However, the leading-order amplitude error depends critically upon α, being negative (indicating stability) if $\alpha = 1$ and positive (indicating instability) if $\alpha = 0$. As shown by Williams (2009), the coefficient of the quadratic term in (15) vanishes if

$$\alpha = \frac{1}{2}, \qquad (16)$$

which implies equal and opposite filter perturbations at the present and future times. With (16) satisfied, (15) becomes

$$|A_P| - 1 = \frac{\nu(4\gamma - 3 + \nu - \nu\gamma)}{4(2 - \nu)^2}(\omega\Delta t)^4 + O[(\omega\Delta t)^6]. \qquad (17)$$

The leading-order amplitude error after taking a single time step now generally scales as $(\Delta t)^4$. Therefore, the leading-order amplitude error compounded over $T/\Delta t$ time steps generally scales as $(\Delta t)^3$, implying third-order amplitude accuracy. The leading-order amplitude error is still approximately proportional to ν for $\nu \ll 1$. However, it now depends critically upon γ, being negative (indicating stability) if $\gamma = 0$ and positive (indicating instability) if $\gamma = 1$. Therefore, a simple method for stabilizing the RAW-filtered leapfrog scheme, while retaining the third-order amplitude accuracy, is to compute the tendency using the unfiltered solution instead of the filtered solution. This method is an alternative to the use of $\alpha \gtrsim \frac{1}{2}$, which stabilizes the scheme but reduces the amplitude accuracy. The coefficient of the quartic term in (17) vanishes if

$$\gamma = \frac{3 - \nu}{4 - \nu}, \qquad (18)$$

which implies that the leapfrog tendency is calculated from a linear combination of the filtered and unfiltered solutions in the ratio $3 - \nu : 1$. In the limit $\nu \to 0$, $\gamma \to \frac{3}{4}$ and the ratio tends to $3 : 1$. With (16) and (18) satisfied, (17) becomes

$$|A_P| - 1 = \frac{\nu}{4(4 - \nu)(2 - \nu)^2}(\omega\Delta t)^6 + O[(\omega\Delta t)^8]. \qquad (19)$$

The leading-order amplitude error after taking a single time step now generally scales as $(\Delta t)^6$. Therefore, the leading-order amplitude error compounded over $T/\Delta t$ time steps generally scales as $(\Delta t)^5$, implying fifth-order

amplitude accuracy. The leading-order amplitude error is still approximately proportional to ν for $\nu \ll 1$. It now has no other parametric dependence, and it is always positive (indicating instability). The coefficient of the sextic term in (19) never vanishes (unless $\nu = 0$, in which case the filter is inactive and the computational mode is undamped).

A series expansion for $\arg(A_P)$ in powers of $\omega\Delta t$ is obtained in the same manner. For α and γ given by (16) and (18), the phase error is found to be

$$\arg(A_P) - \omega\Delta t = \frac{8 + \nu}{12(4 - \nu)}(\omega\Delta t)^3 + O[(\omega\Delta t)^5]. \qquad (20)$$

The leading-order phase error after taking a single time step generally scales as $(\Delta t)^3$. Therefore, the leading-order phase error compounded over $T/\Delta t$ time steps generally scales as $(\Delta t)^2$, implying second-order phase accuracy. The leading-order phase error is relatively insensitive to ν for $\nu \ll 1$. The coefficient of the cubic term in (20) never vanishes (unless $\nu = -8$, in which case the computational mode is amplified). In fact, the phase accuracy is found to be second order for all permissible values of α, γ, and ν, consistent with the general proposition proved by Durran (1991).

c. Behavior for finite $\omega\Delta t$

Section 2b studied the asymptotic behavior of the physical mode as $\omega\Delta t \to 0$. However, the behavior of the physical mode at finite $\omega\Delta t$ is also of great practical interest, as is the behavior of the computational modes. This behavior cannot be obtained from series expansions; therefore, we now study numerical solutions of the cubic equation in (9). We choose $\nu = 0.1$ and $\alpha = \frac{1}{2}$, satisfying (16), and we seek solutions for various values of γ. The behavior of the amplification factors for the case $\gamma = (3 - \nu)/(4 - \nu) \approx 0.744$, which satisfies (18), is shown in Fig. 1. The physical mode is weakly unstable for all values of $\omega\Delta t$, consistent with (19). The usual $2\Delta t$ computational mode (C1) is damped by the filter, and is accompanied by a new $4\Delta t$ computational mode (C2) that is strongly damped.

The behavior when $\gamma = 0$ is shown in Fig. 2. The physical mode is now stable, consistent with (17). The $4\Delta t$ computational mode (C2) is still strongly damped, but the $2\Delta t$ computational mode (C1) becomes unstable for $\omega\Delta t > 0.832$. We infer from Figs. 1 and 2 the existence of an intermediate value of γ between 0 and $(3 - \nu)/(4 - \nu)$, at which the amplification factors for the physical mode and the $2\Delta t$ computational mode meet in the complex plane. In the limit $\nu \to 0$, the intermediate value is $\gamma = \frac{1}{2}$ and the meeting occurs at $\omega\Delta t = 1$. These values may be derived analytically, by first setting
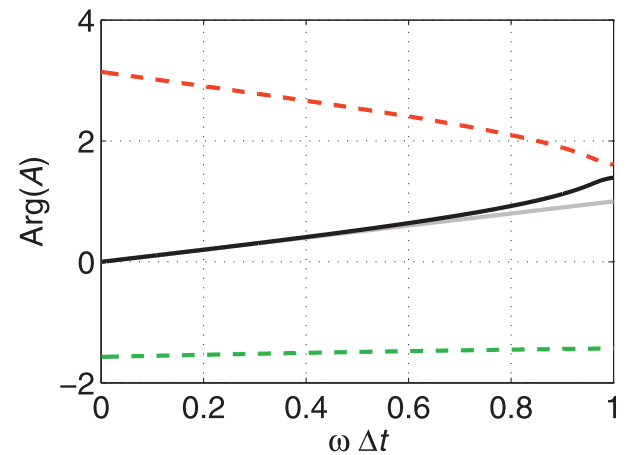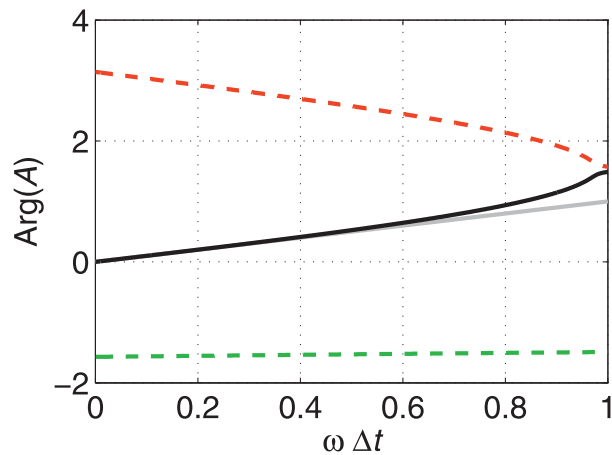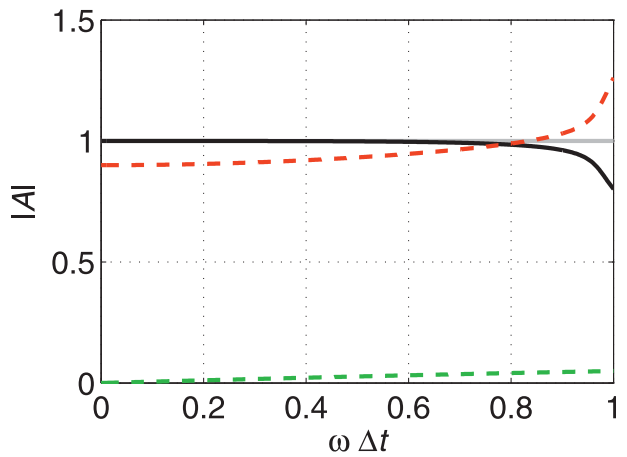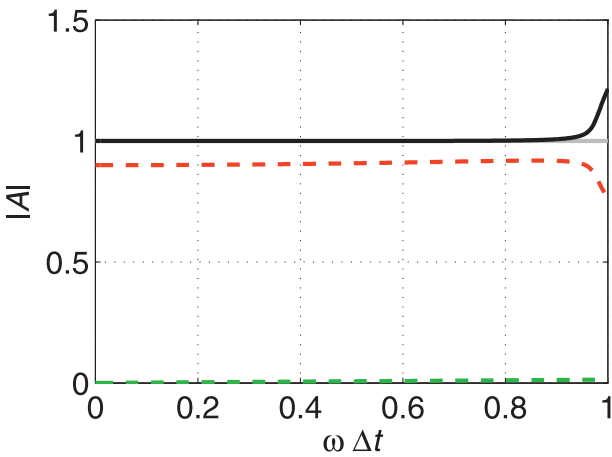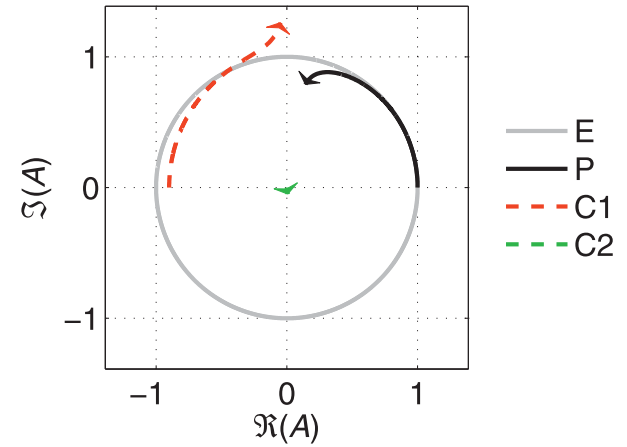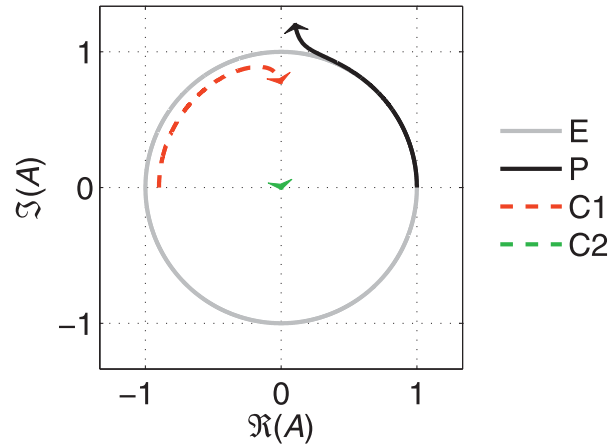
FIG. 1. Complex amplification factors for the RAW-filtered leapfrog scheme with a composite tendency, when applied to the oscillation equation. The scheme is defined by (5)–(7). The roots of (9) are obtained numerically and are plotted here for the case $\nu = 0.1$, $\alpha = \frac{1}{2}$, and $\gamma = (3 - \nu)/(4 - \nu) \approx 0.744$. The physical mode (P) and the computational modes (C1 and C2) are traced as $\omega\Delta t$ increases from 0 to 1. The unit circle, on which the exact amplification factor (E) lies, is also shown.

FIG. 2. As in Fig. 1, but for the case $\nu = 0.1$, $\alpha = \frac{1}{2}$, and $\gamma = 0$.

$\nu = 0$ in (13) to make c_0 vanish and yield a quadratic equation, and by then setting $\nu = 0$ in the real and imaginary parts of the condition for a double root ($c_2^2 = 4c_3c_1$). The behavior when $\gamma = \frac{1}{2}$ is shown in Fig. 3. All three modes are stable unless $\omega\Delta t > 0.975$.
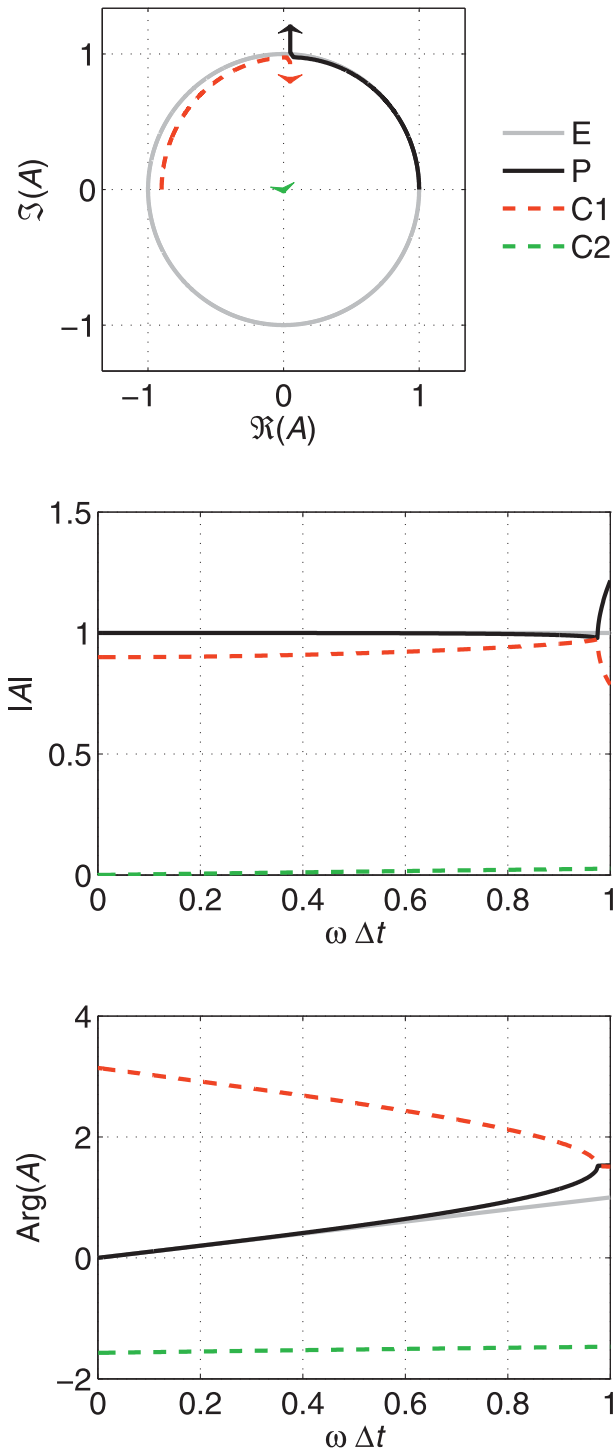
FIG. 3. As in Fig. 1, but for the case $\nu = 0.1$, $\alpha = \frac{1}{2}$, and $\gamma = \frac{1}{2}$.

A summary of the amplitude errors of the physical mode, for $\nu = 0.1$ and various combinations of α and γ, is shown in Fig. 4. The Robert–Asselin filter ($\alpha = 1$) is the most damping case and is stable for $\omega \Delta t < 0.951$. The RAW filter with equal-and-opposite perturbations and

with the leapfrog tendency calculated purely from the filtered solution ($\alpha = \frac{1}{2}$, $\gamma = 1$) is more accurate but is unstable for all $\omega \Delta t$. The use of unequal perturbations ($\alpha = 0.7$, $\gamma = 1$) makes the scheme stable for $\omega \Delta t < 0.871$ and gives errors that are smaller than those of the Robert–Asselin filter. Retaining the equal-and-opposite perturbations but calculating the leapfrog tendency purely from the unfiltered solution ($\alpha = \frac{1}{2}$, $\gamma = 0$) also stabilizes the scheme, but the damping is relatively strong and a computational mode is stable only for $\omega \Delta t < 0.832$. Calculating the leapfrog tendency from a particular blend of the filtered and unfiltered solutions [$\alpha = \frac{1}{2}$, $\gamma = (3 - \nu)/(4 - \nu)$] gives the smallest errors but is weakly unstable. The best case is arguably the use of equal-and-opposite filter perturbations, with the leapfrog tendency calculated from an equal blend of the filtered and unfiltered solutions ($\alpha = \frac{1}{2}$, $\gamma = \frac{1}{2}$). This scheme has relatively small errors and relatively weak damping. The scheme is stable for $\omega \Delta t < 0.975$, which is the best stability limit of all the schemes in the figure, and which is very close to the stability limit of the unfiltered leapfrog scheme ($\omega \Delta t < 1$).

The amplification factors shown in Fig. 4 quantify the amplitude errors associated with taking a single time step. In practical applications, what is of greater interest is the amplitude errors that accumulate over a given integration interval, composed of many time steps. The amplification factors compounded over one complete oscillation period are shown in Fig. 5. The errors are magnified compared to those for a single time step, and the magnification is greater for smaller values of $\omega \Delta t$ because more steps are required to complete an oscillation. If an error tolerance is specified, such as the amplitude being permitted to grow or decay by no more than 0.5% per oscillation, then maximum time steps may be read off from the figure, by locating where the compound amplification factors first reach 0.995 or 1.005.

Can further accuracy improvements be achieved by using in the leapfrog calculation a composite representation of the solution at the past time, in addition to a composite representation of the tendency at the present time? This scheme would be achieved by replacing $\bar{\bar{x}}_{n-1}$ in (3) with a linear combination of the three available numerical solutions: $\bar{\bar{x}}_{n-1}$, $\bar{x}_{n-1}$, and x_{n-1}. Two new weighting parameters would be introduced. This scheme has been analyzed by the author, and the results are reported briefly here. A new degree of freedom is introduced into the numerical scheme, making the polynomial equation for the amplification factor quartic, and yielding a physical mode and three computational modes. Series expansions show that no further improvement is obtained to the amplitude or phase errors, for any permissible values of the two new weighting parameters.
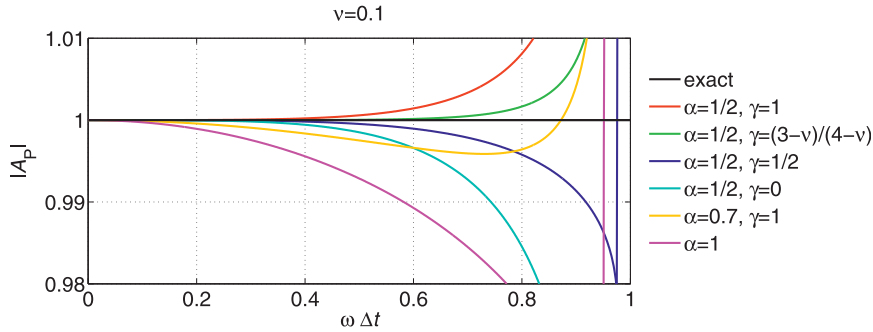
FIG. 4. Magnitudes of the complex amplification factors for the physical mode of the RAW-filtered leapfrog scheme with a composite tendency, when applied to the oscillation equation. The scheme is defined by (5)–(7). The roots of (9) are obtained numerically and are plotted for the case $\nu = 0.1$, for various combinations of α and γ. Curves are plotted only where all computational modes are stable. Note that when $\alpha = 1$, γ vanishes from the numerical scheme (see text).

Therefore, the accuracy is affected by the use of a composite tendency, but not by the use of a composite starting point for the leapfrog extrapolation.

3. A more discriminating filter

a. The numerical scheme

The Robert–Asselin and RAW filters damp the computational mode by introducing a form of diffusion into the numerical solution. The introduction of diffusion is evident from (6) and (7), in which the $(1, -2, 1)$ coefficients in the expressions for the filter perturbations represent a discrete approximation to the second time derivative. In particular, they represent a first-order backward-difference approximation to the second time derivative at time $n + 1$, or a second-order centered-difference approximation to the second time derivative at time n.

In space–time problems, biharmonic diffusion (∇^4) is more effective than Laplacian diffusion (∇^2) at damping

shortwave grid-scale noise relative to longwave resolved features. By analogy, in leapfrog integrations with a diffusive filter, we anticipate that fourth-derivative time diffusion (d^4/dt^4) will be more effective than second-derivative time diffusion (d^2/dt^2) at damping the fast computational mode relative to the slow physical mode. To quantify this expectation, suppose that the angular frequencies of the two modes are ω_{fast} and ω_{slow}, respectively. Then the factor by which the computational mode is damped more strongly than the physical mode is $(\omega_{\text{fast}}/\omega_{\text{slow}})^2$ for second-derivative time diffusion, but $(\omega_{\text{fast}}/\omega_{\text{slow}})^4$ for fourth-derivative time diffusion.

Motivated by the above discussion, let us attempt to improve the composite-tendency leapfrog scheme of section 2. We will study the effects of a more discriminating variant of the RAW filter, in which the second-derivative time diffusion is replaced with fourth-derivative time diffusion. This is achieved by retaining (5) without modification, but replacing (6) and (7) with
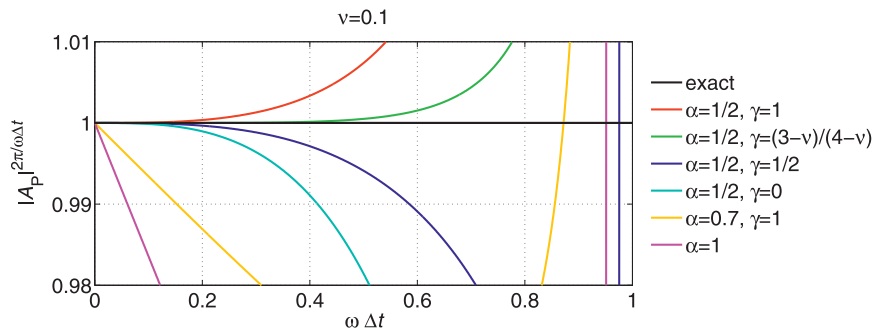

FIG. 5. As in Fig. 4, except that here the amplification factors are not for a single time step but for one complete period of the oscillation. This is achieved by raising $|A_{\text{P}}|$ to the power of the number of time steps per period, which is $2\pi/(\omega\Delta t)$.

$$\overline{\overline{x}}_n = \overline{x}_n + \nu\alpha(\overline{\overline{x}}_{n-3} - 4\overline{\overline{x}}_{n-2} + 6\overline{\overline{x}}_{n-1} - 4\overline{x}_n + x_{n+1}),$$
(21)

$$\overline{x}_{n+1} = x_{n+1} - \nu(1-\alpha)$$
$$\times (\overline{\overline{x}}_{n-3} - 4\overline{\overline{x}}_{n-2} + 6\overline{\overline{x}}_{n-1} - 4\overline{x}_n + x_{n+1}).$$
(22)

The $(1, -4, 6, -4, 1)$ coefficients in the expressions for the filter perturbations represent a discrete approximation to the fourth time derivative. In particular, they represent a first-order backward-difference approximation to the fourth time derivative at time $n + 1$, or a second-order centered-difference approximation to the fourth time derivative at time $n - 1$. Note that a factor of ½ was included in the expressions for the filter perturbations in (6) and (7), so that ν could be interpreted as the fraction by which the $(1, -2, 1)$ filter nudges the present state toward the mean of the past and future states. No such interpretation is possible for the $(1, -4, 6, -4, 1)$ filter, and so the corresponding factor of ½ is omitted from (21) and (22). Combining (3), (21), and (22) into a single equation for the numerical scheme demonstrates that the overall truncation error is $O[(\omega\Delta t)^2]$ for all values of ν, α, and γ. Note in particular that, unlike with the $(1, -2, 1)$ filter, the choice $\alpha \neq$ ½ does not degrade the overall accuracy from second order to first order.

Proceeding as in section 2, we apply the numerical scheme defined by (5), (21), and (22) to the oscillation equation in (4). Again, the determinant of a 3×3 matrix of coefficients must vanish, yielding a quintic equation for the amplification factor:

$$d_5A^5 + d_4A^4 + d_3A^3 + d_2A^2 + d_1A + d_0 = 0,$$
(23)

where

$$d_5 = 1,$$
(24)

$$d_4 = -\nu(4 + 3\alpha) - 2[1 - \nu(1-\alpha)\gamma]i\omega\Delta t,$$
(25)

$$d_3 = -1 + \nu(7 + \alpha) + \nu[8(1-\alpha)(1-\gamma) + 12\alpha]i\omega\Delta t,$$
(26)

$$d_2 = -\nu(4 - 3\alpha) - \nu[12(1-\alpha)(1-\gamma) + 8\alpha]i\omega\Delta t,$$
(27)

$$d_1 = \nu(1-\alpha) + \nu[8(1-\alpha)(1-\gamma) + 2\alpha]i\omega\Delta t,$$
(28)

$$d_0 = -2\nu(1-\alpha)(1-\gamma)i\omega\Delta t.$$
(29)

Equation (23) generally yields five roots for $A(\nu, \alpha, \gamma, i\omega\Delta t)$. In addition to the physical mode, hereafter labeled P, there are generally four computational modes, hereafter labeled C1, C2, C3, and C4. However, for the same reasons as in section 2, when $\nu = 0$, $\alpha = 1$, or $\gamma = 1$, the quintic equation reduces to a quartic equation (because $d_0 = 0$) and one of the computational modes vanishes.

b. Behavior as $\omega\Delta t \to 0$

A series expansion for $|A_P|$ in powers of $\omega\Delta t$ gives the amplitude error to be

$$|A_P| - 1 = -\frac{\nu(1 - 2\alpha)}{2(1 - \nu - 2\alpha\nu)}(\omega\Delta t)^4 + O[(\omega\Delta t)^6].$$
(30)

The leading-order amplitude error after taking a single time step generally scales as $(\Delta t)^4$. Therefore, the leading-order amplitude error compounded over $T/\Delta t$ time steps generally scales as $(\Delta t)^3$, implying third-order amplitude accuracy. The leading-order amplitude error is approximately proportional to ν for $\nu \ll 1$ and is independent of γ. However, the leading-order amplitude error depends critically upon α, being negative (indicating stability) if $\alpha = 0$ and positive (indicating instability) if $\alpha = 1$. The coefficient of the quartic term in (30) vanishes if

$$\alpha = \frac{1}{2},$$
(31)

which is the same condition on α that was obtained for the $(1, -2, 1)$ filter. With (31) satisfied, (30) becomes

$$|A_P| - 1 = \frac{\nu(5 - 8\gamma - 9\nu + 14\nu\gamma)}{8(1 - 2\nu)^2}(\omega\Delta t)^6 + O[(\omega\Delta t)^8].$$
(32)

The leading-order amplitude error after taking a single time step now generally scales as $(\Delta t)^6$. Therefore, the leading-order amplitude error compounded over $T/\Delta t$ time steps generally scales as $(\Delta t)^5$, implying fifth-order amplitude accuracy. The leading-order amplitude error is still approximately proportional to ν for $\nu \ll 1$. However, it now depends critically upon γ, being negative (indicating stability) if $\gamma = 1$ and positive (indicating instability) if $\gamma = 0$. The coefficient of the sextic term in (32) vanishes if

$$\gamma = \frac{5 - 9\nu}{2(4 - 7\nu)},$$
(33)

which implies that the leapfrog tendency is calculated from a linear combination of the filtered and unfiltered solutions in the ratio $5 - 9\nu : 3 - 5\nu$. This ratio differs from the corresponding ratio obtained for the $(1, -2, 1)$ filter. In the limit $\nu \to 0$, $\gamma \to$ ⅝ and the ratio tends to $5 : 3$. The optimal value of γ becomes zero when $\nu = $ ⅝,

but this value of ν corresponds to far stronger filtering than is used in practice. With (31) and (33) satisfied, (32) becomes

$$|A_P| - 1 = -\frac{5\nu(4 - 13\nu + 11\nu^2)}{32(1 - 2\nu)^2(4 - 7\nu)}(\omega\Delta t)^8 + O[(\omega\Delta t)^{10}].$$

(34)

The leading-order amplitude error after taking a single time step now generally scales as $(\Delta t)^8$. Therefore, the leading-order amplitude error compounded over $T/\Delta t$ time steps generally scales as $(\Delta t)^7$, implying seventh-order amplitude accuracy. The leading-order amplitude error is still approximately proportional to ν for $\nu \ll 1$. It now has no other parametric dependence, and it is always negative (indicating stability). The coefficient of the octic term in (34) never vanishes (unless $\nu = 0$, in which case the filter is inactive and the computational mode is undamped).

A series expansion for $\arg(A_P)$ in powers of $\omega\Delta t$ is obtained in the same manner. For α and γ given by (31) and (33), the phase error is found to be

$$\arg(A_P) - \omega\Delta t = \frac{1}{6}(\omega\Delta t)^3 + O[(\omega\Delta t)^5].$$ (35)

The leading-order phase error after taking a single time step generally scales as $(\Delta t)^3$. Therefore, the leading-order phase error compounded over $T/\Delta t$ time steps generally scales as $(\Delta t)^2$, implying second-order phase accuracy. The leading-order phase error is independent of ν. The coefficient of the cubic term in (35) never vanishes.

c. Behavior for finite $\omega\Delta t$

To examine the behavior at finite $\omega\Delta t$, we now study numerical solutions of the quintic equation in (23). We choose $\nu = 0.1$ and $\alpha = \frac{1}{2}$, satisfying (31), and we seek solutions for $\gamma = (5 - 9\nu)/[2(4 - 7\nu)] \approx 0.621$, which satisfies (33). The behavior of the amplification factors is shown in Fig. 6. The physical mode is stable for all values of $\omega\Delta t$, consistent with (34). Of the four computational modes, three (C2, C3, and C4) are stable for all values of $\omega\Delta t$, but one (C1) becomes unstable for $\omega\Delta t > 0.616$. As $\nu \to 0$, C1 and C2 tend to $2\Delta t$ modes, C3 tends to a stationary mode, and C4 tends to a $4\Delta t$ mode (not shown).

A summary of the amplitude errors of the physical mode, for $\nu = 0.1$ and various combinations of α and γ, is shown in Fig. 7. The use of unequal filter perturbations ($\alpha = 1$ or $\alpha = 0$) gives the largest errors. The errors are reduced by the use of equal-and-opposite perturbations ($\alpha = \frac{1}{2}$) with noncomposite tendencies ($\gamma = 0$ or $\gamma = 1$),
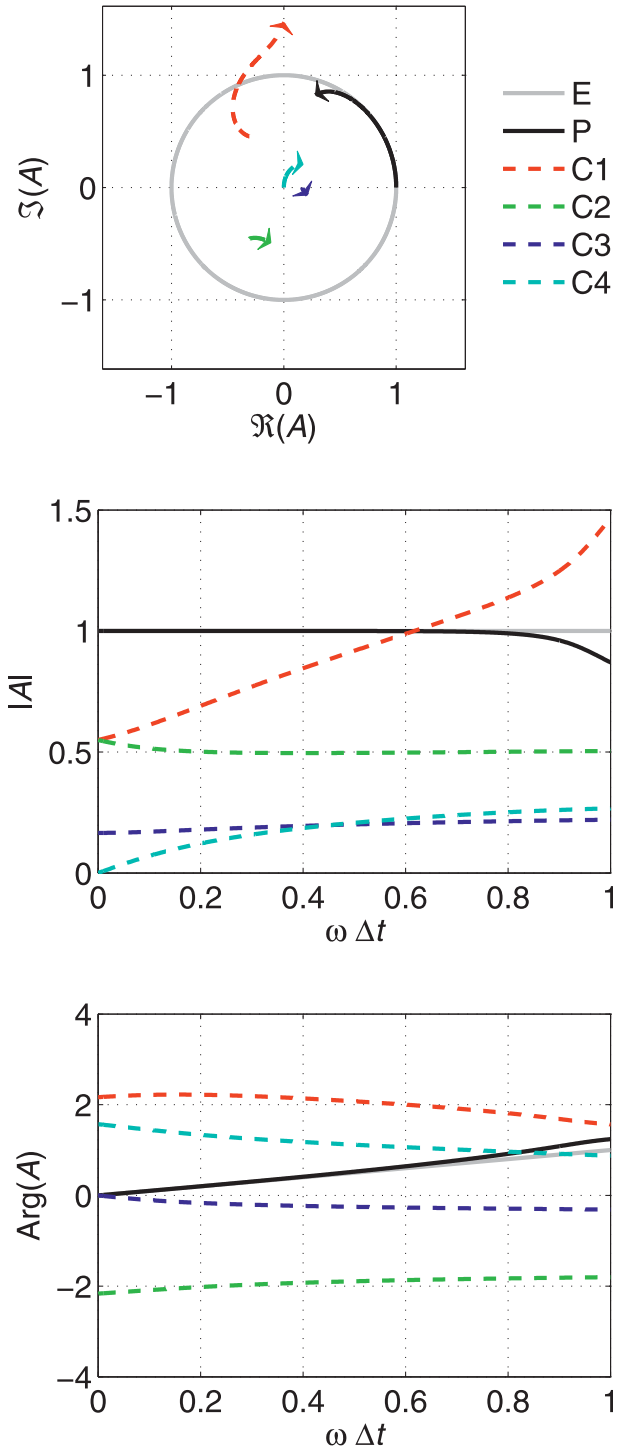

FIG. 6. Complex amplification factors for the (1, −4, 6, −4, 1)-filtered leapfrog scheme with a composite tendency, when applied to the oscillation equation. The scheme is defined by (5), (21), and (22). The roots of (23) are obtained numerically and are plotted here for the case $\nu = 0.1$, $\alpha = \frac{1}{2}$, and $\gamma = (5 - 9\nu)/[2(4 - 7\nu)] \approx 0.621$. The physical mode (P) and the computational modes (C1, C2, C3, and C4) are traced as $\omega\Delta t$ increases from 0 to 1. The unit circle, on which the exact amplification factor (E) lies, is also shown.
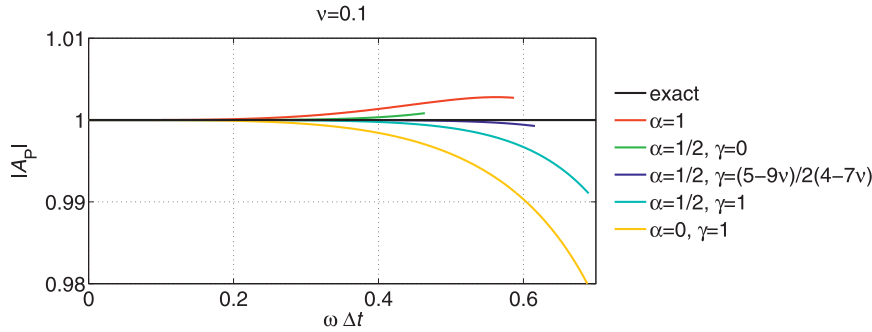
FIG. 7. Magnitudes of the complex amplification factors for the physical mode of the $(1, -4, 6, -4, 1)$-filtered leapfrog scheme with a composite tendency, when applied to the oscillation equation. The scheme is defined by (5), (21), and (22). The roots of (23) are obtained numerically and are plotted for the case $\nu = 0.1$, for various combinations of α and γ. Curves are plotted only where all computational modes are stable. Note that when $\alpha = 1$, γ vanishes from the numerical scheme (see text).

and they are reduced even further with a composite tendency $\{\gamma = (5 - 9\nu)/[2(4 - 7\nu)]\}$. However, unstable computational modes generally constrain $\omega\Delta t$ more strongly with the $(1, -4, 6, -4, 1)$ filter than with the $(1, -2, 1)$ filter. The amplification factors compounded over one complete oscillation period are shown in Fig. 8.

4. Test integrations

To complement the linear analyses performed in sections 2 and 3, the proposed schemes will now be tested in numerical integrations of a simple nonlinear system. A bob of unit mass attached to the end of a rigid massless pendulum of unit length in a unit gravitational field oscillates at an angle of $x(t)$ to the downward vertical according to

$$\frac{dx}{dt} = v, \tag{36}$$

$$\frac{dv}{dt} = -\sin x. \tag{37}$$

The total (kinetic plus gravitational potential) energy of the pendulum, relative to the total energy when at rest in the stable equilibrium position, is

$$E = 1 - \cos x + \frac{1}{2}v^2. \tag{38}$$

The total energy is conserved by the continuous equations, which give $dE/dt = 0$, and so it is of interest to determine whether energy is created or destroyed spuriously by the numerical schemes.

Equations (36) and (37) are integrated starting from $x = 0.95\pi$ and $v = 0$, corresponding to the bob being released from rest at an angle of 9° from the upward vertical. These are challenging initial conditions for a numerical scheme, because the nonlinearities are large and the oscillating bob comes to rest close to the unstable equilibrium position directly above the point of suspension. In each integration, a single first-order Euler forward step is done to initialize the leapfrog scheme. In the integrations using the $(1, -4, 6, -4, 1)$ filter, two initial applications of the $(1, -2, 1)$ filter are used to
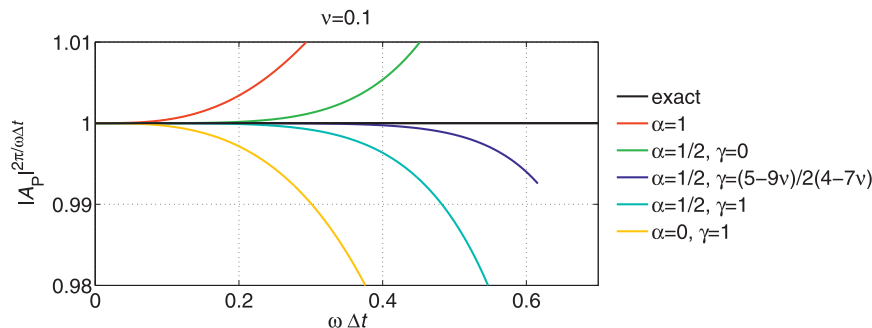

FIG. 8. As in Fig. 7, except that here the amplification factors are not for a single time step but for one complete period of the oscillation. This is achieved by raising $|A_P|$ to the power of the number of time steps per period, which is $2\pi/(\omega\Delta t)$.
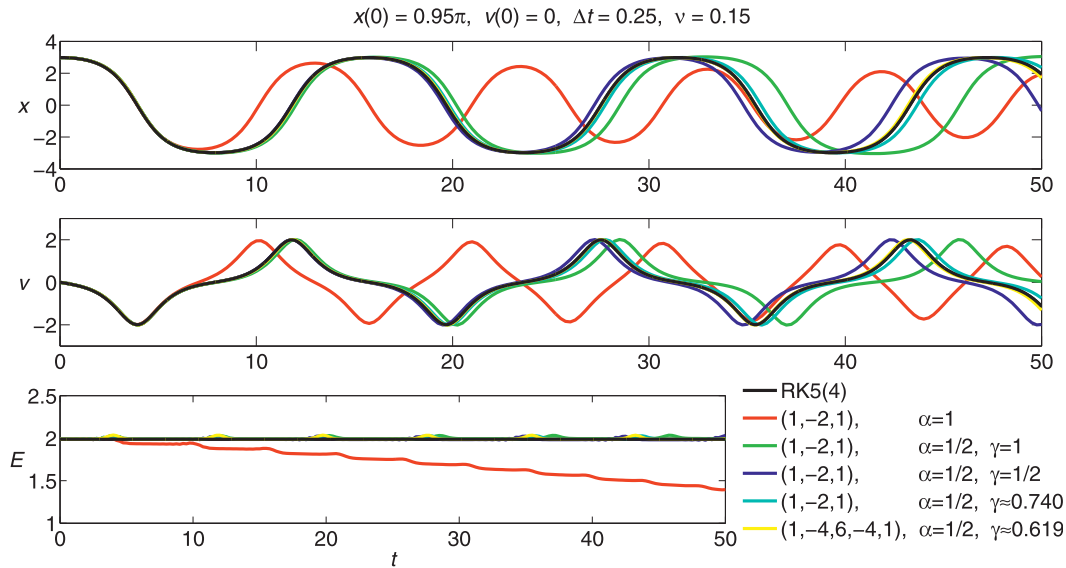
FIG. 9. Filtered leapfrog integrations of the nonlinear pendulum equations, compared to an RK5(4) integration that may be taken to be exact. The initial conditions at $t = 0$ are $x = 0.95\pi$ and $v = 0$. The time step is $\Delta t = 0.25$ and the filter parameter is $\nu = 0.15$. Note that when $\alpha = 1$, γ vanishes from the numerical scheme (see text).

generate a long enough history to start applying the $(1, -4, 6, -4, 1)$ filter. Both x and v are filtered after each leapfrog step. The filter strength is chosen to be relatively large ($\nu = 0.15$) to emphasize the effects of the filters. The time step is $\Delta t = 0.25$.

The filtered leapfrog integrations are compared to a highly accurate reference solution, which is computed using an explicit adaptive Runge–Kutta method [RK5(4)] known as the Dormand–Prince (DOPRI) method (Dormand and Prince 1980). This method involves taking a fifth-order step to estimate the error associated with taking a fourth-order step, and then using the error to adapt the step size. For the adaptivity criterion applied to both x and v, the relative error tolerance is 10^{-12} and the absolute error tolerance is 10^{-15}. The estimated error in each integration step is less than the larger of two quantities: the relative error tolerance multiplied by the state, and the absolute error tolerance.

The results are shown in Fig. 9. The first leapfrog solution to depart visibly from the reference solution is the one using the $(1, -2, 1)$ filter with $\alpha = 1$, which is the original Robert–Asselin filter with first-order amplitude accuracy. The oscillations are too rapid, because the filter quickly damps the excursions, and the oscillation frequency of the nonlinear pendulum increases as the amplitude decreases. The next two leapfrog solutions to depart visibly from the reference solution are the ones using the $(1, -2, 1)$ filter with $\alpha = \frac{1}{2}$ and either $\gamma = 1$ or $\gamma = \frac{1}{2}$, which both have third-order amplitude accuracy and are a substantial improvement. However, the higher-order schemes proposed in this paper remain

close to the reference solution for even longer. The leapfrog solution using the $(1, -2, 1)$ filter with $\alpha = \frac{1}{2}$ and $\gamma = (3 - \nu)/(4 - \nu) \approx 0.740$, which has fifth-order amplitude accuracy, has only slightly departed from the reference solution after three full oscillations, despite the relatively strong filtering. The leapfrog solution using the $(1, -4, 6, -4, 1)$ filter with $\alpha = \frac{1}{2}$ and $\gamma = (5 - 9\nu)/[2(4 - 7\nu)] \approx 0.619$, which has seventh-order amplitude accuracy, is even better and lies the closest to the reference solution for the longest time. The energy conservation property of the time-continuous equations appears to be preserved adequately by all the filtered leapfrog schemes except the one using the Robert–Asselin filter, which rapidly removes energy from the system.

5. Summary and discussion

This paper has studied the accuracy and stability of various implementations of filtered leapfrog schemes. The aim was to improve the filtering methods used currently, which, when integrating linear oscillations, have first-order amplitude accuracy (Robert 1966; Asselin 1972) and third-order amplitude accuracy (Williams 2009, 2011). First, leapfrogging over a suitably weighted blend of the filtered and unfiltered tendencies was found to eliminate the third-order amplitude errors and yield fifth-order amplitude accuracy. Then, the use of a more discriminating filter was found to eliminate the fifth-order amplitude errors and yield seventh-order amplitude accuracy. Each of the schemes studied was found

TABLE 1. Summary of the stability and accuracy of the composite-tendency leapfrog scheme proposed in section 2 (upper part) and of the same scheme with a more discriminating filter proposed in section 3 (lower part). The traditional implementation of the Robert–Asselin filter is in the top row. The value of γ is irrelevant if $\alpha = 1$. The number of computational modes is reduced by 1 if $\alpha = 1$ or $\gamma = 1$. The number of function evaluations per time step is 1 if $\gamma = 0$ or $\gamma = 1$ and is 2 otherwise. For the amplitude order of accuracy, parentheses indicate that the amplitude error of the physical mode is positive as $\omega \Delta t \to 0$. The maximum $\omega \Delta t$ for stability is the maximum value at which all the modes (physical and computational) are stable when $\nu = 0.1$. The maximum $\omega \Delta t$ for accuracy is the maximum value at which the amplitude is conserved to within $\pm 0.5\%$ over one oscillation period when $\nu = 0.1$, with parentheses indicating $+0.5\%$ and absence of parentheses indicating -0.5%.

Filter	α	γ	No. of computational modes	No. of function evaluations per time step	Order	Amplitude order of accuracy	Phase order of accuracy	Maximum $\omega \Delta t$ for stability ($\nu = 0.1$)	Maximum $\omega \Delta t$ for accuracy ($\nu = 0.1$)
$(1, -2, 1)$	1	—	1	1	1	1	2	0.951	0.030
$(1, -2, 1)$	1/2	1	1	1	2	(3)	2	0	(0.448)
$(1, -2, 1)$	1/2	$(3 - \nu)/(4 - \nu)$	2	2	2	(5)	2	0	(0.712)
$(1, -2, 1)$	1/2	1/2	2	2	2	3	2	0.975	0.475
$(1, -2, 1)$	1/2	0	2	1	2	3	2	0.832	0.333
$(1, -2, 1)$	0	1	1	1	1	(1)	2	0	(0.030)
$(1, -4, 6, -4, 1)$	1	—	3	1	2	(3)	2	0	(0.228)
$(1, -4, 6, -4, 1)$	1/2	1	3	1	2	5	2	0.690	0.424
$(1, -4, 6, -4, 1)$	1/2	$(5 - 9\nu)/[2(4 - 7\nu)]$	4	2	2	7	2	0.616	0.586
$(1, -4, 6, -4, 1)$	1/2	0	4	1	2	(5)	2	0	(0.394)
$(1, -4, 6, -4, 1)$	0	1	3	1	2	3	2	0.777	0.240

to have second-order phase accuracy, the same as the unfiltered leapfrog scheme. The proposed new schemes were tested in numerical integrations of a simple non-linear system.

In detail, section 2 showed that the $(1, -2, 1)$ filter with strength parameter ν generally gives amplitude errors that are first order. However, if the filter perturbations are equal and opposite, then the errors generally improve to third order. If, in addition, the leapfrogging is done over a linear combination of the filtered and unfiltered tendencies in the ratio $3 - \nu : 1$, then the errors improve to fifth order. Note that a composite tendency cannot be constructed when the Robert–Asselin filter is used, because only the unfiltered tendency exists at that point of the leapfrog calculation. Therefore, the concept of filtering at the future time as well as the present time, which was the key advance of the RAW filter, is crucial for producing the benefits found in this paper. Section 3 showed that the $(1, -4, 6, -4, 1)$ filter generally gives amplitude errors that are third order. However, if the filter perturbations are equal and opposite, then the errors generally improve to fifth order. If, in addition, the leapfrogging is done over a linear combination of the filtered and unfiltered tendencies in the ratio $5 - 9\nu : 3 - 5\nu$, then the errors improve to seventh order.

It is always the case when constructing a numerical scheme that there are many possible discretizations, each of which is consistent in the sense that it tends to the continuous derivative as the step size tends to zero. It has often been found that taking a linear combination of the consistent discretizations results in a better

scheme than taking any single discretization individually. For example, the construction of the composite leapfrog tendency in section 2 is reminiscent of the construction of the Arakawa (1966) Jacobian for modeling advection in a two-dimensional flow. In that case, of three consistent Jacobian discretizations, only a particular linear combination was found to preserve the conservation properties of the continuous Jacobian. In the present paper, of two consistent filtered leapfrog discretizations, only a particular linear combination is found to eliminate the amplitude errors at a particular order and increase the amplitude accuracy.

A summary of the properties of the proposed new schemes is given in Table 1. For each scheme, the relationship between the order of the overall truncation error in the differential equation and the orders of the amplitude and phase errors satisfies the general proposition of Durran (1991). In particular, although the orders of the amplitude errors vary between the schemes, none of the schemes has a phase error that is better than second order. In terms of the orders of the amplitude and phase errors, several of the second-order schemes in Table 1 are as good as, or better than, the best second-order scheme (Young's method A) in the comprehensive list given by Durran (1991).

Of particular interest are the maximum time steps that may be used if a given error tolerance is specified. For example, suppose it is decided that a loss of amplitude of no more than 0.5% per oscillation may be tolerated. Then, referring to Table 1, the maximum permissible time step in the usual implementation of the

leapfrog scheme with the Robert–Asselin filter ($\alpha = 1$, $\nu = 0.1$) would be $\omega\Delta t = 0.030$. In contrast, the maximum permissible time step in the proposed composite-tendency leapfrog scheme with the RAW filter ($\alpha = \frac{1}{2}$, $\gamma = \frac{1}{2}$, $\nu = 0.1$) would be $\omega\Delta t = 0.475$, which is an order of magnitude greater. Therefore, a substantial reduction in computational expense is achieved, even after taking into account the need for two function evaluations per time step instead of one.

In terms of accuracy across a broad range of $\omega\Delta t$, the best stable scheme in Table 1 is the $(1, -4, 6, -4, 1)$ filter with $\alpha = \frac{1}{2}$ and $\gamma = (5 - 9\nu)/[2(4 - 7\nu)]$. With this scheme, even using a time step as large as $\omega\Delta t = 0.586$, the amplitude will still be conserved to within 0.5% during each oscillation when $\nu = 0.1$. However, the maximum stable time step is only $\omega\Delta t = 0.616$, which is relatively small. In terms of stability across a broad range of $\omega\Delta t$, the best scheme in the table is the $(1, -2, 1)$ filter with $\alpha = \frac{1}{2}$ and $\gamma = \frac{1}{2}$. With this scheme, the maximum stable time step is $\omega\Delta t = 0.975$ when $\nu = 0.1$. Furthermore, the maximum time step for amplitude conservation to within 0.5% during each oscillation is $\omega\Delta t = 0.475$, which is the second-best value in the table. On balance, the $(1, -2, 1)$ filter with $\alpha = \frac{1}{2}$ and $\gamma = \frac{1}{2}$ appears to offer the best combination of stability and accuracy.

Although the amplitude errors in filtered leapfrog schemes have yielded to the methods proposed herein, the phase errors have remained stubborn. However, there may be good physical reasons for valuing amplitude accuracy above phase accuracy. For example, it is the amplitude accuracy that determines the degree of energy conservation by the numerical scheme, at least for linear oscillations. The relative importance of amplitude accuracy and phase accuracy depends on the application. For long-term ocean or climate simulations, good amplitude accuracy may be required to prevent errors caused by numerical damping from accumulating over the long integration periods. Good phase accuracy may be less important, because long-term statistics usually matter more than individual weather systems or ocean eddies. In contrast, for short-term weather simulations, good phase accuracy may be required to correctly predict the evolution of individual weather systems. Good amplitude accuracy may be less important, because the short integration periods do not allow much time for amplitude errors to accumulate. Therefore, the new schemes proposed in this paper, with amplitude accuracies of up to seventh order but phase accuracies limited to second order, may be particularly well suited to ocean and climate applications.

For practical purposes, the computational expense and memory requirement are important considerations when choosing a numerical scheme. The calculation of the composite tendency requires two function evaluations per time step, because the tendency must be calculated for the unfiltered state and the filtered state. This doubles the computational expense of the tendency calculation, which is the most expensive component of contemporary atmosphere and ocean models. In models that use a time step sufficiently below the stability limit, however, the increased accuracy allows a longer time step to be taken for the same error tolerance, tending to offset the increased expense. Note also that there are attractive schemes in Table 1 that do not require a composite tendency, because $\gamma = 0$ or $\gamma = 1$, and therefore the computational expense of the tendency calculation is unchanged. In terms of the memory requirement, holding the unfiltered state in memory until the next time step is more burdensome than immediately overwriting it with the filtered state. Also, the $(1, -4, 6, -4, 1)$ filter requires a longer history to be kept in memory than the $(1, -2, 1)$ filter. Whether the increased memory requirement presents a problem in practical applications remains to be seen.

Could further improvements be made to the amplitude accuracy of the filtered leapfrog scheme? Filters based on time derivatives higher than the fourth would discriminate between the physical and computational modes even more strongly than the $(1, -4, 6, -4, 1)$ filter proposed here. For example, the $(1, -6, 15, -20, 15, -6, 1)$ filter would represent a discrete approximation to the sixth time derivative. Such filters would introduce new computational modes and would require more memory, however, and it is unclear that amplitude accuracy higher than seventh order would confer any tangible benefits. A further option would be to apply both the $(1, -2, 1)$ filter and the $(1, -4, 6, -4, 1)$ filter together in combination. These possibilities are left for future work.

REFERENCES

Amezcua, J., 2012: Advances in sequential data assimilation and numerical weather forecasting: An ensemble transform

Kalman–Bucy filter, a study on clustering in deterministic ensemble square root filters, and a test of a new time stepping scheme in an atmospheric model. Ph.D. thesis, University of Maryland, College Park, 154 pp.

——, E. Kalnay, and P. D. Williams, 2011: The effects of the RAW filter on the climatology and forecast skill of the SPEEDY model. *Mon. Wea. Rev.,* **139,** 608–619.

Arakawa, A., 1966: Computational design for long-term numerical integration of the equations of fluid motion: Two-dimensional incompressible flow. *J. Comput. Phys.,* **1** (1), 119–143.

Asselin, R., 1972: Frequency filter for time integrations. *Mon. Wea. Rev.,* **100,** 487–490.

Bartello, P., 2002: A comparison of time discretization schemes for two-timescale problems in geophysical fluid dynamics. *J. Comput. Phys.,* **179** (1), 268–285.

Clancy, C., and J. A. Pudykiewicz, 2013: A class of semi-implicit predictor–corrector schemes for the time integration of atmospheric models. *J. Comput. Phys.,* **250,** 665–684.

Cordero, E., and A. Staniforth, 2004: A problem with the Robert–Asselin time filter for three-time-level semi-implicit semi-Lagrangian discretizations. *Mon. Wea. Rev.,* **132,** 600–610.

Déqué, M., and D. Cariolle, 1986: Some destabilizing properties of the Asselin time filter. *Mon. Wea. Rev.,* **114,** 880–884.

Dietrich, D. E., and J. J. Wormeck, 1985: An optimized implicit scheme for compressible reactive gas flow. *Numer. Heat Transfer,* **8** (3), 335–348.

Dormand, J. R., and P. J. Prince, 1980: A family of embedded Runge–Kutta formulae. *J. Comput. Appl. Math.,* **6** (1), 19–26.

Durran, D. R., 1991: The third-order Adams–Bashforth method: An attractive alternative to leapfrog time differencing. *Mon. Wea. Rev.,* **119,** 702–720.

——, 1999: *Numerical Methods for Wave Equations in Geophysical Fluid Dynamics.* Springer-Verlag, 465 pp.

——, and P. N. Blossey, 2012: Implicit–explicit multistep methods for fast-wave–slow-wave problems. *Mon. Wea. Rev.,* **140,** 1307–1325.

Fraedrich, K., H. Jansen, E. Kirk, U. Luksch, and F. Lunkeit, 2005: The Planet Simulator: Towards a user friendly model. *Meteor. Z.,* **14** (3), 299–304.

Griffies, S. M., R. C. Pacanowski, M. Schmidt, and V. Balaji, 2001: Tracer conservation with an explicit free surface method for z-coordinate ocean models. *Mon. Wea. Rev.,* **129,** 1081–1098.

Haltiner, G. J., and R. T. Williams, 1980: *Numerical Prediction and Dynamic Meteorology.* 2nd ed. Wiley, 496 pp.

Hartogh, P., A. S. Medvedev, T. Kuroda, R. Saito, G. Villanueva, A. G. Feofilov, A. A. Kutepov, and U. Berger, 2005: Description and climatology of a new general circulation model of the Martian atmosphere. *J. Geophys. Res.,* **110,** E11008, doi:10.1029/2005JE002498.

Heimsund, B.-O., and J. Berntsen, 2004: On a class of ocean model instabilities that may occur when applying small time steps, implicit methods, and low viscosities. *Ocean Modell.,* **7** (1–2), 135–144.

Huang, R. X., and J. Pedlosky, 2003: On aliasing Rossby waves induced by asynchronous time stepping. *Ocean Modell.,* **5** (1), 65–76.

Jablonowski, C., and D. L. Williamson, 2011: The pros and cons of diffusion, filters and fixers in atmospheric general circulation models. *Numerical Techniques for Global Atmospheric Models,* P. H. Lauritzen et al., Eds., Springer, 381–493.

Kalnay, E., 2003: *Atmospheric Modeling, Data Assimilation and Predictability.* Cambridge University Press, 357 pp.

Kurihara, Y., 1965: On the use of implicit and iterative methods for the time integration of the wave equation. *Mon. Wea. Rev.,* **93,** 33–46.

Lilly, D. K., 1965: On the computational stability of numerical solutions of time-dependent nonlinear geophysical fluid dynamics problems. *Mon. Wea. Rev.,* **93,** 11–26.

Magazenkov, L. N., 1980: Time integration schemes for fluid dynamics equations, effectively damping the high frequency components (in Russian). *Tr. Gl. Geofiz. Obs.,* **410,** 120–129.

Maplesoft, 2011: Maple 15. Maplesoft.

Marsaleix, P., F. Auclair, T. Duhaut, C. Estournel, C. Nguyen, and C. Ulses, 2012: Alternatives to the Robert–Asselin filter. *Ocean Modell.,* **41,** 53–66.

Mesinger, F., and A. Arakawa, 1976: *Numerical Methods Used in Atmospheric Models.* Global Atmospheric Research Programme Publications Series, Vol. 17, WMO–ICSU, 70 pp.

Mishra, S. K., and S. Sahany, 2011: Effects of time step size on the simulation of tropical climate in NCAR-CAM3. *Climate Dyn.,* **37,** 689–704.

——, J. Srinivasan, and R. S. Nanjundiah, 2008: The impact of the time step on the intensity of ITCZ in an aquaplanet GCM. *Mon. Wea. Rev.,* **136,** 4077–4091.

Oger, N., O. Pannekoucke, A. Doerenbecher, and P. Arbogast, 2012: Assessing the influence of the model trajectory in the adaptive observation Kalman filter sensitivity method. *Quart. J. Roy. Meteor. Soc.,* **138,** 813–825.

Pfeffer, R. L., I. M. Navon, and X. L. Zou, 1992: A comparison of the impact of two time-differencing schemes on the NASA GLAS climate model. *Mon. Wea. Rev.,* **120,** 1381–1393.

Ren, D., and L. M. Leslie, 2011: Three positive feedback mechanisms for ice-sheet melting in a warming climate. *J. Glaciol.,* **57** (206), 1057–1066.

Roache, P. J., and D. E. Dietrich, 1988: Evaluation of the filtered leapfrog–trapezoidal time integration method. *Numer. Heat Transfer,* **14** (2), 149–164.

Robert, A. J., 1966: The integration of a low order spectral form of the primitive meteorological equations. *J. Meteor. Soc. Japan,* **44,** 237–245.

——, and M. Lépine, 1997: An anomaly in the behaviour of a time filter used with the leapfrog scheme in atmospheric models. *Numerical Methods in Atmospheric and Oceanic Modelling: The André J. Robert Memorial Volume,* C. A. Lin, R. Laprise, and H. Ritchie, Eds., NRC Research Press, S3–S15.

Schlesinger, R. E., L. W. Uccellini, and D. R. Johnson, 1983: The effects of the Asselin time filter on numerical solutions to the linearized shallow-water wave equations. *Mon. Wea. Rev.,* **111,** 455–467.

Tandon, M. K., 1987: Robert's recursive frequency filter: A reexamination. *Meteor. Atmos. Phys.,* **37** (1), 48–59.

Teixeira, J., C. A. Reynolds, and K. Judd, 2007: Time step sensitivity of nonlinear atmospheric models: Numerical convergence, truncation error growth, and ensemble design. *J. Atmos. Sci.,* **64,** 175–189.

Watanabe, M., and Coauthors, 2010: Improved climate simulation by MIROC5: Mean states, variability, and climate sensitivity. *J. Climate,* **23,** 6312–6335.

Williams, P. D., 2009: A proposed modification to the Robert–Asselin time filter. *Mon. Wea. Rev.,* **137,** 2538–2546.

——, 2011: The RAW filter: An improvement to the Robert–Asselin filter in semi-implicit integrations. *Mon. Wea. Rev.,* **139,** 1996–2007.

——, T. W. N. Haine, P. L. Read, S. R. Lewis, and Y. H. Yamazaki, 2009: QUAGMIRE v1.3: A quasi-geostrophic model for investigating rotating fluids experiments. *Geosci. Model Dev.,* **2** (1), 13–32.

Williamson, D. L., and J. G. Olson, 2003: Dependence of aqua-planet simulations on time step. *Quart. J. Roy. Meteor. Soc.,* **129,** 2049–2064.

Young, C.-C., Y.-H. Tseng, M.-L. Shen, Y.-C. Liang, M.-H. Chen, and C.-H. Chien, 2012: Software development of the TaIwan Multi-scale Community Ocean Model (TIMCOM). *Environ. Modell. Software,* **38,** 214–219.

——, Y.-C. Liang, Y.-H. Tseng, and C.-H. Chow, 2013: Charac-teristics of the RAW filtered leapfrog time-stepping scheme in the ocean general circulation model. *Mon. Wea. Rev.,* in press.

Young, J. A., 1968: Comparative properties of some time differ-encing schemes for linear and nonlinear oscillations. *Mon. Wea. Rev.,* **96,** 357–364.

Zhao, B., and Q. Zhong, 2009: The dynamical and climate tests of an atmospheric general circulation model using the second-order Adams–Bashforth method. *Acta Meteor. Sin.,* **23** (6), 738–749.